ADVANCED MATERIALS
www.advmat.de

Phase-Change Hyperbolic Heterostructures for Nanopolaritonics: A Case Study of hBN/VO_2

Siyuan Dai, Jiawei Zhang, Qiong Ma, Salinporn Kittiwatanakul, Alex McLeod, Xinzhong Chen, Stephanie Gilbert Corder, Kenji Watanabe, Takashi Taniguchi, Jiwei Lu, Qing Dai, Pablo Jarillo-Herrero, Mengkun Liu,* and D. N. Basov**

Unlike conventional plasmonic media, polaritonic van der Waals (vdW) materials hold promise for active control of light–matter interactions. The dispersion relations of elementary excitations such as phonons and plasmons can be tuned in layered vdW systems via stacking using functional substrates. In this work, infrared nanoimaging and nanospectroscopy of hyperbolic phonon polaritons are demonstrated in a novel vdW heterostructure combining hexagonal boron nitride (hBN) and vanadium dioxide (VO_2). It is observed that the insulator-to-metal transition in VO_2 has a profound impact on the polaritons in the proximal hBN layer. In effect, the real-space propagation of hyperbolic polaritons and their spectroscopic resonances can be actively controlled by temperature. This tunability originates from the effective change in local dielectric properties of the VO_2 sublayer in the course of the temperature-tuned insulator-to-metal phase transition. The high susceptibility of polaritons to electronic phase transitions opens new possibilities for applications of vdW materials in combination with strongly correlated quantum materials.

Van der Waals (vdW) materials[1–3] exhibit enigmatic electronic, optical, and magnetic properties. For example, they host Dirac[4] and valley[5] electrons, support unconventional superconductivity,[6,7] exhibit low-dimensional ferromagnetism,[8,9] and harbor topologically protected electronic states.[10,11] Stacking vdW materials into heterostructures offers a versatile and interesting route to control novel material properties and quantum phenomena.[3] This is especially the case when vdW systems are combined with phase-change materials (PCMs),[12–17] which serve as the basis for numerous applications such as energy storage[18,19] and reconfigurable electronics.[20]

In this work, we demonstrate tunable phonon polaritonic behavior in a vdW heterostructure (**Figure 1**a) combining hexagonal boron nitride (hBN) and a representative PCM, vanadium dioxide (VO_2).[21–23] Polaritons[22,24] are hybrid light–matter modes involving collective oscillations of electromagnetic dipoles. In hBN, hyperbolic phonon polaritons (HPPs)[21,25–31] are supported in both type I ($\varepsilon_z < 0$, $\varepsilon_t > 0$) and type II ($\varepsilon_z > 0$, $\varepsilon_t < 0$) regions. The hyperbolic response[32] originates from highly anisotropic mid-infrared (mid-IR) phonon resonances.[24–27,33–35] This natural hyperbolicity in hBN offer advantages over its metamaterial counterparts[32,36] owing to the high light-momentum cutoff set by the interatomic spacing in hBN lattices.[35,37] Therefore, hyperbolicity in hBN holds promise for

Prof. S. Dai
Materials Research and Education Center
Department of Mechanical Engineering
Auburn University
Auburn, Alabama 36849, USA
E-mail: sdai@auburn.edu
J. Zhang, X. Chen, Dr. S. N. G. Corder, Prof. M. Liu
Department of Physics
Stony Brook University
Stony Brook, NY 11794, USA
E-mail: mengkun.liu@stonybrook.edu
Dr. Q. Ma, Prof. P. Jarillo-Herrero
Department of Physics
Massachusetts Institute of Technology
Cambridge, MA 02215, USA
Prof. S. Kittiwatanakul, Prof. J. Lu
Department of Materials Science and Engineering
University of Virginia
Charlottesville, VA 22904, USA
Prof. S. Kittiwatanakul
Department of Physics
Faculty of Science
Chulalongkorn University
Bangkok 10330, Thailand
Dr. A. McLeod, Prof. D. N. Basov
Department of Physics
Columbia University
New York, NY 10027, USA
E-mail: db3056@columbia.edu
Dr. K. Watanabe, Dr. T. Taniguchi
National Institute for Materials Science
Namiki 1-1, Tsukuba, Ibaraki 305-0044, Japan
Prof. Q. Dai
Division of Nanophotonics
CAS Center for Excellence in Nanoscience
National Center for Nanoscience and Technology
Beijing 100190, P. R. China

The ORCID identification number(s) for the author(s) of this article can be found under https://doi.org/10.1002/adma.201900251.

DOI: 10.1002/adma.201900251

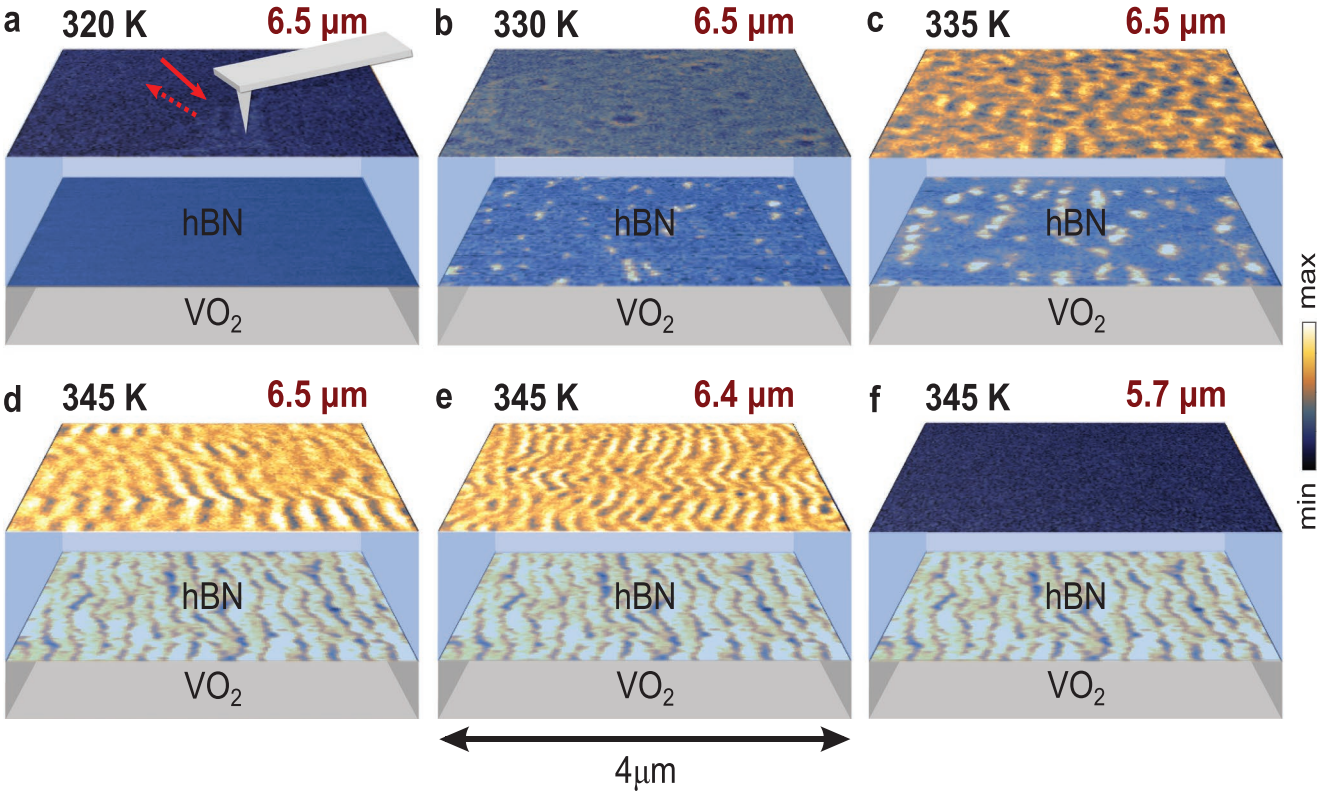

Figure 1. a–f) s-SNOM nanoimages reveal the HPPs and IMT phase transition in hBN/VO_2 heterostructures. s-SNOM images of HPPs (plotted on the hBN top surface) affected by the IMT (hBN/VO_2 interface) recorded at temperatures and incident IR wavelengths of: a) 320 K and 6.5 μm, b) 330 K and 6.5, c) 335 K and 6.5 μm, d) 345 K and 6.5 μm, e) 345 K and 6.4 μm, and f) 345 K and 6.7 μm. Thickness of the hBN: 73 nm.

applications to subdiffractional focusing,[35,37] emission engineering,[38] and light steering[21,30,36] at a microscopic scale. Here, using infrared (IR) near-field nanoscopy, we reveal the dynamic tuning of HPPs by introducing thermal phase transitions in correlated electron materials. We find that HPPs in hBN can be effectively redirected in real space through their interaction with the emerging metallic phase domains in VO_2. The corresponding phonon resonances in type I and type II regions can be switched on and off, respectively, with increasing temperature. We remark that although optical switching of surface phonon polaritons in PCMs has been previously reported in $Ge_3Sb_2Te_6$,[39] the dynamic tuning of the HPPs is unprecedented.

Scattering-type scanning near-field optical microscopy (s-SNOM) is employed to study the hBN/VO_2 heterostructures. We illuminate the tip of an atomic force microscope (AFM) with IR quantum cascade lasers (QCLs: solid red arrow, Figure 1a) and collect the back-scattered IR signal (dashed red arrow). The scattered signal is demodulated at higher harmonics of the tip tapping frequency to yield essentially a near-field signal. The s-SNOM records optical signals with a spatial resolution of 10 nm (see the Experimental Section) and has been extensively used to investigate nano-optical phenomena, including polaritons in vdW materials[21,25,40,41] and phase inhomogeneity in quantum materials.[42,43] The VO_2 film studied in this work had a thickness of 50 nm and was deposited on a $[110]_R$ TiO_2 substrate to ensure a large conductivity jump (five orders of magnitude) during the insulator-to-metal phase transition (IMT).[42] This particular VO_2/TiO_2 system provides a unidirectional metal–insulator phase separation that serves as a unique platform for modulating the dielectric environment of hBN.[44]

The $[110]_R$ VO_2 undergoes an anisotropic IMT over the temperature range from 320 to 345 K.[42] The evolution of the IMT can be characterized by s-SNOM: from the homogenous insulating state to metallic nucleation clusters, and finally unidirectional metallic stripes. These different stages of the IMT with increasing temperature are plotted on the surface of VO_2 (below hBN) in Figure 1a–d. We note that the IMT is nondispersive in the mid-IR frequencies, since identical images were obtained regardless of the IR frequency (Figure 1d–f).

In heterostructures with hBN on top of VO_2, HPPs can be effectively launched by an s-SNOM tip.[21,35,37,45,46] The metal–insulator phase boundaries in VO_2 act as effective reflectors for HPPs. At the beginning of the IMT, ring-shaped polariton fringes appear on the hBN top surface (Figure 1b). This is because the metallic nucleation sites (MNS) in VO_2 are point-like at low temperature, and the standing-wave interference between the MNS-reflected and tip-launched HPPs forms rings around the MNS. At higher temperatures, these polariton fringes start to connect with each other as the density of MNS increases (335 K, Figure 1c). At temperatures above 335 K, metallic stripes emerge in VO_2, and the corresponding HPP fringes exhibit a similar stripe contrast with illumination wavelength $\lambda_{IR} = 6.5$ μm (Figure 1d).

At $\lambda_{IR} = 6.4$ μm (Figure 1e), the polariton fringes become narrower, indicating a shorter HPP wavelength, which is in accord

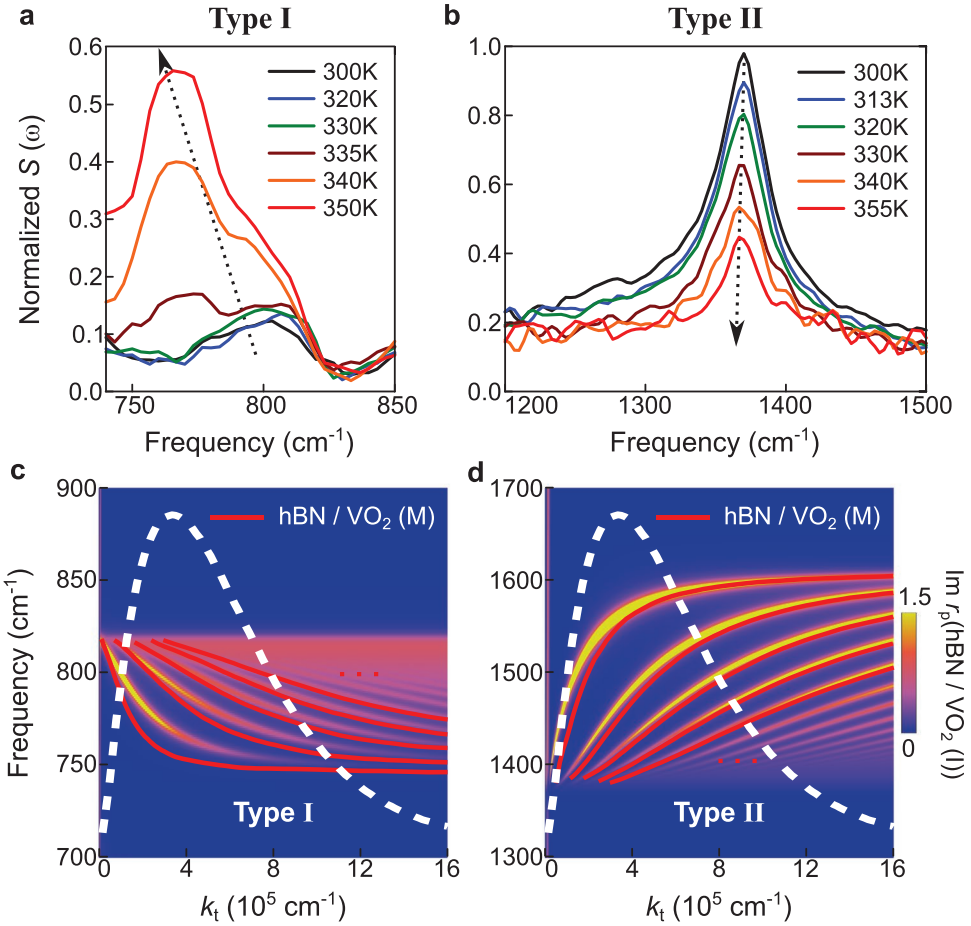

Figure 2. Tuning HPPs in hBN/VO_2 heterostructures by temperature control. a,b), Nano-FTIR spectra of hBN/VO_2 at various temperatures in type I (a) and type II (b) hyperbolic regions. c,d) Simulation of hybridization between HPPs and IMT in hBN/VO_2 heterostructures in type I (a) and type II (b) hyperbolic regions. The polariton dispersion is plotted by red curves in the metallic state and with false color in the insulating state of VO_2. The white dashed curves indicate the near-field coupling weight function. Nano-FTIR spectra resolution: 3.33 cm^{-1}. hBN thickness: 73 nm.

with the frequency–momentum dispersion of HPPs.[25,27] The hybrid polariton phase-transition is further verified in a control experiment: no evident nano-optical features can be observed at the wavelength $\lambda_{IR} = 5.7$ µm (Figure 1f), which is outside of the hyperbolic regime. In comparison with previously demonstrated topographic reflectors/launchers for nanopolaritons,[25,40,41,47] the conducting stripes in VO_2 are predominantly electronic reflectors, which do not reveal any evident topographic features in AFM measurements. The reflection of HPPs in this work can be attributed to local permittivity variations that are formed "electronically" at the phase boundaries in VO_2.

Having established the interaction between polaritons in hBN and the IMT in VO_2, we now demonstrate the dynamic tuning of the phonon resonances by performing Fourier transform infrared nanospectroscopy (nano-FTIR) of the hBN/VO_2 heterostructure. The nano-FTIR spectra were obtained near the center of the hBN flakes, away from the edges where strong variations of the signal intensity were caused by polaritonic standing waves. The phonon spectral peaks in the low-frequency (type I) and high-frequency (type II) regions are demonstrated in **Figure 2**a,b, respectively. At room temperature, the spectral features are consistent with the reported results in hBN/SiO_2 structures.[34] As the temperature increases, interesting spectral evolutions in the heterostructure of hBN/VO_2 can be observed in both type I and type II regions. In the type I region (Figure 2a), the spectral intensity of the *z*-axis phonon increases as VO_2 undergoes the IMT with increasing temperature. In the type II region (Figure 2b), in contrast, the spectral intensity of the in-plane phonon decreases with increasing temperature. The intensity of the nano-FTIR spectrum in type I and type II regions exhibits opposite trends with increasing temperature. Furthermore, the frequency of the phonon resonances in the type I region redshift during the IMT from 803 cm^{-1} (black curve in Figure 2a) to 766 cm^{-1} (red curve in Figure 2a). Therefore, both the intensity and the peak frequency of the hBN phonon resonance can be tuned by temperature-controlled IMT in VO_2.

The tuning of phonon resonances stems from the modification of hyperbolic polariton dispersion in hBN/VO_2 heterostructures. We account for this effect by performing a simulation of frequency (ω)–momentum (k_t) dispersion (Figure 2c,d) in hBN/VO_2. Although a quantitative interpretation requires a precise measurement of the local permittivity at each temperature which may demand future work, our ω–k_t dispersion simulation can qualitatively account for all the main observations in Figure 2a,b.

Since nano-FTIR probes spectroscopic response with an in-plane momentum k_t that is effectively coupled to the s-SNOM tip, its spectra manifest optical modes within a finite momentum region. This tip-coupled momentum is scoped by the time-averaged near-field coupling weight function[48] $G = \langle k_t^2 e^{-2k_t z_d} \rangle_t$ (white dashed curves in Figure 2c,d). Here z_d is the distance between the sample surface and the AFM probe, which is modeled as a point dipole.[48] In hBN, multiple branches of HPPs (shown as false color in Figure 2c,d) in type I and type II regions contribute to the z-axis and in-plane phonon resonance, respectively (300 K, black curves in Figure 2a,b). In the simulation, the permittivity of hBN was obtained from ref. [26]. The VO_2 is modeled as a variable-dielectric ground plane, in which the complex dielectric constants in the fully insulating and metallic phases are extracted from previous experiments.[49] As VO_2 undergoes the IMT, type I HPP modes shift into the strong-coupling region (white dashed curves), whereas in the type II region, HPP modes shift out. This is evident on comparing the ω–k_t dispersion of hBN on insulating VO_2 (false color in Figure 2c,d) with that of hBN on metallic VO_2 (red curves in Figure 2c,d). During the IMT, coupling between the s-SNOM probe with more polaritonic modes can account for the increasing spectral intensity in the type I region. In contrast, coupling with fewer polaritonic modes in the type II region will cause a decrease in the spectral intensity. Moreover, with increasing metallicity, the hybrid HPP-IMT modes are redshifted in both type I and type II regions, in accordance with our experimental observations at increasing temperature (Figure 2a,b). Note that while HPPs shift in the course of the IMT (e.g., see dispersion plots in Figure 2c,d), no evident mode broadening was observed (Section S1, Supporting Information). This is an interesting observation since losses of proximal layers are considered to be important for the dynamics of plasmon polaritons (close cousins of HPPs) in graphene based heterostructures.[50,51] Here, in contrast, the metallicity of VO_2 does not generate noticeable mode broadening, which can be attributed to the fact that HPPs travel mostly through the bulk of the hBN slabs.

In summary, nanoimaging and nanospectroscopy augmented with frequency–momentum dispersion analysis reveal effective tuning of phonon polaritons in hBN/VO_2 heterostructures. Dynamic redirection of polariton waves can be achieved at the nanoscale using metallic nucleations in VO_2 as electronic reflectors, where delicate control of the local dielectric environment is readily available.[52,53] We envision the possibility of engineering local patterns[39,54] in PCMs for memory applications in polaritonic circuits and other advanced nanophotonic devices.[55] Furthermore, the methodology that we have utilized here can be easily extended to the tuning of nanopolaritons in heterostructures combining PCMs with other vdW materials, including graphene,[56] transition metal dichalcogenides,[12] topological insulators,[57] and black phosphorus,[58] where the polaritonic modes are also sensitive to the dielectric surroundings. In addition, multiple routes for tuning the IMT, including electrostatic, electrochemical, and ultrafast switching, can all be utilized to control polaritons in hBN/VO_2 heterostructures.

During the preparation of this manuscript, we became aware of another experimental work on phonon polaritons in hBN/VO_2 heterostructures.[59]

Experimental Section

Experimental Setup: The IR nanoimaging and nano-FTIR experiments on hBN/VO_2 heterostructures were performed using s-SNOM. A commercial s-SNOM system (www.neaspec.com) is used based on a tapping-mode AFM and a commercial AFM tip (tip radius ≈ 10 nm) with a $PtIr_5$ coating. In the experiment, the AFM tip is illuminated by monochromatic QCLs (www.daylightsolutions.com) and a broadband source from a difference frequency generation system (www.lasnix.com) to cover a frequency range of 900–2300 cm^{-1}. The s-SNOM nanoimages were recorded by a pseudo-heterodyne interferometric detection module with an AFM tapping frequency of 280 kHz and a tapping amplitude around 70 nm. To remove the background signal, the s-SNOM output signal was demodulated at the third harmonics of the tapping frequency.

Sample Fabrication: The VO_2 substrates studied in this report were deposited on $[110]_R$ TiO_2 substrates (1 cm × 1 cm) by temperature-optimized sputtering using reactive-bias ion-beam deposition in a mixed Ar and O_2 atmosphere. These substrates showed consistently anisotropic THz and DC conductivity.[42] A 1–2% tensile strain along the c_R axis was present in these substrates owing to the lattice mismatch between TiO_2 and VO_2. The hBN crystals were mechanically exfoliated onto the VO_2/TiO_2 substrates.

Supporting Information

Supporting Information is available from the Wiley Online Library or from the author.

Acknowledgements

S.D. and J.Z. contributed equally to this work. Work at Columbia University on optical phenomena in vdW materials is supported by DOE-BES DE-FG02-00ER45799 and Betty Moore Foundation's EPiQS Initiative through Grant GBMF4533. Q.M. and P.J.-H. were supported by the Center for Excitonics, an Energy Frontier Research Center funded by the DOE, Office of Science, BES under Award Number DESC0001088 and AFOSR Grant FA9550-16-1-0382, as well as the Gordon and Betty Moore Foundation's EPiQS Initiative through Grant GBMF4541 to P.J.-H.

Conflict of Interest

The authors declare no conflict of interest.

Keywords

hexagonal boron nitride, phase-change materials, polaritons

Received: January 12, 2019
Revised: February 26, 2019
Published online: March 25, 2019

[1] A. K. Geim, I. V. Grigorieva, *Nature* **2013**, *499*, 419.
[2] K. S. Novoselov, A. Mishchenko, A. Carvalho, A. H. Castro Neto, *Science* **2016**, *353*, aac9439.
[3] D. N. Basov, R. D. Averitt, D. Hsieh, *Nat. Mater.* **2017**, *16*, 1077.
[4] A. H. Castro Neto, F. Guinea, N. M. R. Peres, K. S. Novoselov, A. K. Geim, *Rev. Mod. Phys.* **2009**, *81*, 109.
[5] X. Xu, W. Yao, D. Xiao, T. F. Heinz, *Nat. Phys.* **2014**, *10*, 343.

[6] Y. Cao, V. Fatemi, S. Fang, K. Watanabe, T. Taniguchi, E. Kaxiras, P. Jarillo-Herrero, *Nature* **2018**, *556*, 43.
[7] M. A. Subramanian, C. C. Torardi, J. C. Calabrese, J. Gopalakrishnan, K. J. Morrissey, T. R. Askew, R. B. Flippen, U. Chowdhry, A. W. Sleight, *Science* **1988**, *239*, 1015.
[8] C. Gong, L. Li, Z. Li, H. Ji, A. Stern, Y. Xia, T. Cao, W. Bao, C. Wang, Y. Wang, Z. Q. Qiu, R. J. Cava, S. G. Louie, J. Xia, X. Zhang, *Nature* **2017**, *546*, 265.
[9] B. Huang, G. Clark, E. Navarro-Moratalla, D. R. Klein, R. Cheng, K. L. Seyler, D. Zhong, E. Schmidgall, M. A. McGuire, D. H. Cobden, W. Yao, D. Xiao, P. Jarillo-Herrero, X. Xu, *Nature* **2017**, *546*, 270.
[10] M. Z. Hasan, C. L. Kane, *Rev. Mod. Phys.* **2010**, *82*, 3045.
[11] X.-L. Qi, S.-C. Zhang, *Rev. Mod. Phys.* **2011**, *83*, 1057.
[12] Y. Wang, J. Xiao, H. Zhu, Y. Li, Y. Alsaid, K. Y. Fong, Y. Zhou, S. Wang, W. Shi, Y. Wang, A. Zettl, E. J. Reed, X. Zhang, *Nature* **2017**, *550*, 487.
[13] Y. Cao, V. Fatemi, A. Demir, S. Fang, S. L. Tomarken, J. Y. Luo, J. D. Sanchez-Yamagishi, K. Watanabe, T. Taniguchi, E. Kaxiras, R. C. Ashoori, P. Jarillo-Herrero, *Nature* **2018**, *556*, 80.
[14] M. D. Goldflam, G.-X. Ni, K. W. Post, Z. Fei, Y. Yeo, J. Y. Tan, A. S. Rodin, B. C. Chapler, B. Özyilmaz, A. H. Castro Neto, M. M. Fogler, D. N. Basov, *Nano Lett.* **2015**, *15*, 4859.
[15] J. Momand, F. R. L. Lange, R. Wang, J. E. Boschker, M. A. Verheijen, R. Calarco, M. Wuttig, B. J. Kooi, *J. Mater. Res.* **2016**, *31*, 3115.
[16] J. Kalikka, X. Zhou, J. Behera, G. Nannicini, R. E. Simpson, *Nanoscale* **2016**, *8*, 18212.
[17] Q. Wang, E. T. F. Rogers, B. Gholipour, C.-M. Wang, G. Yuan, J. Teng, N. I. Zheludev, *Nat. Photonics* **2016**, *10*, 60.
[18] A. Sharma, V. V. Tyagi, C. R. Chen, D. Buddhi, *Renewable Sustainable Energy Rev.* **2009**, *13*, 318.
[19] M. Wuttig, N. Yamada, *Nat. Mater.* **2007**, *6*, 824.
[20] M. Wuttig, H. Bhaskaran, T. Taubner, *Nat. Photonics* **2017**, *11*, 465.
[21] A. J. Giles, S. Dai, O. J. Glembocki, A. V. Kretinin, Z. Sun, C. T. Ellis, J. G. Tischler, T. Taniguchi, K. Watanabe, M. M. Fogler, K. S. Novoselov, D. N. Basov, J. D. Caldwell, *Nano Lett.* **2016**, *16*, 3858.
[22] T. Low, A. Chaves, J. D. Caldwell, A. Kumar, N. X. Fang, P. Avouris, T. F. Heinz, F. Guinea, L. Martin-Moreno, F. Koppens, *Nat. Mater.* **2017**, *16*, 182.
[23] M. Liu, A. J. Sternbach, D. N. Basov, *Rep. Prog. Phys.* **2017**, *80*, 014501.
[24] D. N. Basov, M. M. Fogler, F. J. García de Abajo, *Science* **2016**, *354*, aag1992.
[25] S. Dai, Z. Fei, Q. Ma, A. S. Rodin, M. Wagner, A. S. McLeod, M. K. Liu, W. Gannett, W. Regan, K. Watanabe, T. Taniguchi, M. Thiemens, G. Dominguez, A. H. C. Neto, A. Zettl, F. Keilmann, P. Jarillo-Herrero, M. M. Fogler, D. N. Basov, *Science* **2014**, *343*, 1125.
[26] E. Yoxall, M. Schnell, A. Y. Nikitin, O. Txoperena, A. Woessner, M. B. Lundeberg, F. Casanova, L. E. Hueso, F. H. L. Koppens, R. Hillenbrand, *Nat. Photonics* **2015**, *9*, 674.
[27] J. D. Caldwell, A. V. Kretinin, Y. Chen, V. Giannini, M. M. Fogler, Y. Francescato, C. T. Ellis, J. G. Tischler, C. R. Woods, A. J. Giles, M. Hong, K. Watanabe, T. Taniguchi, S. A. Maier, K. S. Novoselov, *Nat. Commun.* **2014**, *5*, 5221.
[28] X. G. Xu, B. G. Ghamsari, J.-H. Jiang, L. Gilburd, G. O. Andreev, C. Zhi, Y. Bando, D. Golberg, P. Berini, G. C. Walker, *Nat. Commun.* **2014**, *5*, 4782.
[29] A. J. Giles, S. Dai, I. Vurgaftman, T. Hoffman, S. Liu, L. Lindsay, C. T. Ellis, N. Assefa, I. Chatzakis, T. L. Reinecke, J. G. Tischler, M. M. Fogler, J. H. Edgar, D. N. Basov, J. D. Caldwell, *Nat. Mater.* **2017**, *17*, 134.
[30] P. Li, I. Dolado, F. J. Alfaro-Mozaz, F. Casanova, L. E. Hueso, S. Liu, J. H. Edgar, A. Y. Nikitin, S. Vélez, R. Hillenbrand, *Science* **2018**, *359*, 892.
[31] A. Ambrosio, M. Tamagnone, K. Chaudhary, L. A. Jauregui, P. Kim, W. L. Wilson, F. Capasso, *Light: Sci. Appl.* **2018**, *7*, 27.
[32] A. Poddubny, I. Iorsh, P. Belov, Y. Kivshar, *Nat. Photonics* **2013**, *7*, 948.
[33] Z. Zheng, J. Chen, Y. Wang, X. Wang, X. Chen, P. Liu, J. Xu, W. Xie, H. Chen, S. Deng, N. Xu, *Adv. Mater.* **2018**, *30*, 1705318.
[34] S. Dai, Q. Ma, M. K. Liu, T. Andersen, Z. Fei, M. D. Goldflam, M. Wagner, K. Watanabe, T. Taniguchi, M. Thiemens, F. Keilmann, G. C. A. M. Janssen, S. E. Zhu, P. Jarillo Herrero, M. M. Fogler, D. N. Basov, *Nat. Nanotechnol.* **2015**, *10*, 682.
[35] P. Li, M. Lewin, A. V. Kretinin, J. D. Caldwell, K. S. Novoselov, T. Taniguchi, K. Watanabe, F. Gaussmann, T. Taubner, *Nat. Commun.* **2015**, *6*, 7507.
[36] A. A. High, R. C. Devlin, A. Dibos, M. Polking, D. S. Wild, J. Perczel, N. P. de Leon, M. D. Lukin, H. Park, *Nature* **2015**, *522*, 192.
[37] S. Dai, Q. Ma, T. Andersen, A. S. McLeod, Z. Fei, M. K. Liu, M. Wagner, K. Watanabe, T. Taniguchi, M. Thiemens, F. Keilmann, P. Jarillo-Herrero, M. M. Fogler, D. N. Basov, *Nat. Commun.* **2015**, *6*, 6963.
[38] H. N. S. Krishnamoorthy, Z. Jacob, E. Narimanov, I. Kretzschmar, V. M. Menon, *Science* **2012**, *336*, 205.
[39] P. Li, X. Yang, T. W. W. Maß, J. Hanss, M. Lewin, A.-K. U. Michel, M. Wuttig, T. Taubner, *Nat. Mater.* **2016**, *15*, 870.
[40] J. Chen, M. Badioli, P. Alonso-Gonzalez, S. Thongrattanasiri, F. Huth, J. Osmond, M. Spasenovic, A. Centeno, A. Pesquera, P. Godignon, A. Zurutuza Elorza, N. Camara, F. J. G. de Abajo, R. Hillenbrand, F. H. L. Koppens, *Nature* **2012**, *487*, 77.
[41] Z. Fei, A. S. Rodin, G. O. Andreev, W. Bao, A. S. McLeod, M. Wagner, L. M. Zhang, Z. Zhao, M. Thiemens, G. Dominguez, M. M. Fogler, A. H. C. Neto, C. N. Lau, F. Keilmann, D. N. Basov, *Nature* **2012**, *487*, 82.
[42] M. K. Liu, M. Wagner, E. Abreu, S. Kittiwatanakul, A. McLeod, Z. Fei, M. Goldflam, S. Dai, M. M. Fogler, J. Lu, S. A. Wolf, R. D. Averitt, D. N. Basov, *Phys. Rev. Lett.* **2013**, *111*, 096602.
[43] M. M. Qazilbash, M. Brehm, B.-G. Chae, P.-C. Ho, G. O. Andreev, B.-J. Kim, S. J. Yun, A. V. Balatsky, M. B. Maple, F. Keilmann, H.-T. Kim, D. N. Basov, *Science* **2007**, *318*, 1750.
[44] M. Liu, M. Wagner, J. Zhang, A. McLeod, S. Kittiwatanakul, Z. Fei, E. Abreu, M. Goldflam, A. J. Sternbach, S. Dai, K. G. West, J. Lu, S. A. Wolf, R. D. Averitt, D. N. Basov, *Appl. Phys. Lett.* **2014**, *104*, 121905.
[45] S. Dai, Q. Ma, Y. Yang, J. Rosenfeld, M. D. Goldflam, A. McLeod, Z. Sun, T. I. Andersen, Z. Fei, M. Liu, Y. Shao, K. Watanabe, T. Taniguchi, M. Thiemens, F. Keilmann, P. Jarillo-Herrero, M. M. Fogler, D. N. Basov, *Nano Lett.* **2017**, *17*, 5285.
[46] S. Dai, M. Tymchenko, Y. Yang, Q. Ma, M. Pita-Vidal, K. Watanabe, T. Taniguchi, P. Jarillo-Herrero, M. M. Fogler, A. Alù, D. N. Basov, *Adv. Mater.* **2018**, *30*, 1706358.
[47] P. Alonso-González, A. Y. Nikitin, F. Golmar, A. Centeno, A. Pesquera, S. Vélez, J. Chen, G. Navickaite, F. Koppens, A. Zurutuza, F. Casanova, L. E. Hueso, R. Hillenbrand, *Science* **2014**, *344*, 1369.
[48] Z. Fei, G. O. Andreev, W. Bao, L. M. Zhang, A. S. McLeod, C. Wang, M. K. Stewart, Z. Zhao, G. Dominguez, M. Thiemens, M. M. Fogler, M. J. Tauber, A. H. Castro-Neto, C. N. Lau, F. Keilmann, D. N. Basov, *Nano Lett.* **2011**, *11*, 4701.
[49] M. M. Qazilbash, M. Brehm, G. O. Andreev, A. Frenzel, P. C. Ho, B.-G. Chae, B.-J. Kim, S. J. Yun, H.-T. Kim, A. V. Balatsky, O. G. Shpyrko, M. B. Maple, F. Keilmann, D. N. Basov, *Phys. Rev. B* **2009**, *79*, 075107.
[50] A. Woessner, M. B. Lundeberg, Y. Gao, A. Principi, P. Alonso-González, M. Carrega, K. Watanabe, T. Taniguchi, G. Vignale, M. Polini, J. Hone, R. Hillenbrand, F. H. L. Koppens, *Nat. Mater.* **2015**, *14*, 421.
[51] G. X. Ni, A. S. McLeod, Z. Sun, L. Wang, L. Xiong, K. W. Post, S. S. Sunku, B. Y. Jiang, J. Hone, C. R. Dean, M. M. Fogler, D. N. Basov, *Nature* **2018**, *557*, 530.
[52] J. Duan, R. Chen, J. Li, K. Jin, Z. Sun, J. Chen, *Adv. Mater.* **2017**, *29*, 1702494.

[53] S. Dai, J. Quan, G. Hu, C. Qiu, T. H. Tao, X. Li, A. Alù, *Nano Lett.* **2019**, *19*, 1009.
[54] S. N. Gilbert Corder, X. Chen, S. Zhang, F. Hu, J. Zhang, Y. Luan, J. A. Logan, T. Ciavatti, H. A. Bechtel, M. C. Martin, M. Aronson, H. S. Suzuki, S.-i. Kimura, T. Iizuka, Z. Fei, K. Imura, N. K. Sato, T. H. Tao, M. Liu, *Nat. Commun.* **2017**, *8*, 2262.
[55] A. F. Koenderink, A. Alù, A. Polman, *Science* **2015**, *348*, 516.
[56] A. Vakil, N. Engheta, *Science* **2011**, *332*, 1291.
[57] P. Di Pietro, M. Ortolani, O. Limaj, A. Di Gaspare, V. Giliberti, F. Giorgianni, M. Brahlek, N. Bansal, N. Koirala, S. Oh, P. Calvani, S. Lupi, *Nat. Nanotechnol.* **2013**, *8*, 556.
[58] A. Nemilentsau, T. Low, G. Hanson, *Phys. Rev. Lett.* **2016**, *116*, 066804.
[59] T. G. Folland, A. Fali, S. T. White, J. R. Matson, S. Liu, N. A. Aghamiri, J. H. Edgar, R. F. Haglund, Y. Abate, J. D. Caldwell, *Nat. Commun.* **2018**, *9*, 4371.